Journal of Power Sources 193 (2009) 754–760

Contents lists available at ScienceDirect

Journal of Power Sources

journal homepage: www.elsevier.com/locate/jpowsour

Three-dimensional anode engineering for the direct methanol fuel cell

A. Bauer*, C.W. Oloman, E.L. Gyenge

Department of Chemical and Biological Engineering, The University of British Columbia, 2360 East Mall, Vancouver, BC, Canada V6T 1Z3

ARTICLE INFO

Article history:
Received 12 March 2009
Received in revised form 22 April 2009
Accepted 23 April 2009
Available online 3 May 2009

Keywords:
Electrode design
Experimental design
Direct methanol fuel cell (DMFC)
Platinum
Porous electrodes

ABSTRACT

Catalyzed graphite felt three-dimensional anodes were investigated in direct methanol fuel cells (DMFCs) operated with sulfuric acid supporting electrolyte. With a conventional serpentine channel flow field the preferred anode thickness was 100 μm, while a novel flow-by anode showed the best performance with a thickness of 200–300 μm. The effects of altering the methanol concentration, anolyte flow rate and operating temperature on the fuel cell superficial power density were studied by full (2^3+1) factorial experiments on a cell with anode area of 5 cm^2 and excess oxidant O_2 at 200 kPa(abs). For operation in the flow-by mode with 2 M methanol at 2 $cm^3\ min^{-1}$ and 353 K the peak power density was 2380 $W\ m^{-2}$ with a PtRuMo anode catalyst, while a PtRu catalyst yielded 2240 $W\ m^{-2}$ under the same conditions.

1. Introduction

Conventional direct methanol fuel cells (DMFCs) have a design similar to that employed for hydrogen fuel cells, in which the anodes consist of a catalyst layer and a gas diffusion layer (Fig. 1). The catalyst layer is typically prepared by spraying or brushing a catalyst ink onto the gas diffusion layer (gas diffusion electrode, GDE) or onto the proton exchange membrane (catalyst coated membrane, CCM) [1].

The DMFC is normally fueled by an aqueous liquid solution of methanol that sometimes includes a supporting electrolyte. Fuel is fed to the conventional DMFC through flow field channels incorporated in the end plate and penetrates the diffusion layer to the electro-active catalyst layer, where methanol is oxidized or may cross the membrane and interfere with the cathode reaction [2,3]. Carbon dioxide generated by the electro-oxidation of methanol at the catalyst/electrolyte interface is transported by diffusion and/or convection back to the flow field for discharge in 2-phase flow with the liquid anolyte, along with unreacted methanol and intermediates such as formic acid. This carbon dioxide in the gas phase can impair the fuel cell performance by increasing the Ohmic resistance and blocking mass transfer pathways.

The crossover of methanol and the disengagement of CO_2 gas from the anode are important issues in DMFC design that have been studied over the last decade. Several techniques have been investigated to deal with methanol crossover. In early work it was shown that crossover can be suppressed by distributing electrocatalyst through a multi-layer porous anode which is fed with the methanol solution from a flow field on the face opposite that in contact with the membrane [4]. More recently attempts have been made to reduce crossover by increasing the anolyte viscosity [5], or by obstructing the membrane with inert materials like silica [6–8]. With respect to gas disengagement in conventional GDE electrodes the studies include, for example:

- applying hydrophobic PTFE coatings to the gas diffusion layer [9,10];
- increasing the anolyte liquid load to compress and disperse gas bubbles [11];
- adding PTFE to the catalyst layer [12];
- changing the configuration of the anode flow field and manifold [13].

Some of these approaches involve trade-offs that compromise the anode function. For example, increasing the PTFE loading of the anode catalyst layer improved gas disengagement but diminished both the electronic and ionic conductivities [12].

Alternative electrode designs have been presented for improving the performance of DMFCs by providing a high surface area support material to allow for depositing high surface area catalysts and/or increased porosity to improve CO_2 disengagement. The results of some laboratory studies of alternative anode designs are summarized in Table 1.

The alternative anode designs in Table 1 include the use of PtRu catalysts on supports ranging from a titanium mesh [14,15] to carbon nanotubes and nanocoils [16,17] and nanoporous carbon

* Corresponding author. Tel.: +1 604 827 3418; fax: +1 604 822 6003.
E-mail address: a.bauer@chml.ubc.ca (A. Bauer).

0378-7753/$ – see front matter © 2009 Elsevier B.V. All rights reserved.
doi:10.1016/j.jpowsour.2009.04.054

Nomenclature

abs	absolute (referring to pressure)
a_s	specific area [$m^2\,m^{-3}$]
c	methanol concentration [M]
CCM	catalyst coated membrane
d_f	diameter of single fiber [m]
DMFC	direct methanol fuel cell
E_{cell}	fuel cell potential [V]
E^o	standard potential at 298 K [V]
f	electrolyte fraction in total electrode volume
F	Flow rate (of methanol solution, unless stated otherwise) [$cm^3\,min^{-1}$]
GDE	gas diffusion electrode
i	superficial current density [$A\,m^{-2}$]
MEA	membrane electrode assembly
p	(peak) superficial power density [$W\,m^{-2}$]
S	standard conditions (101 kPa(abs), 273 K)
SEM	scanning electron microscopy
SFF	serpentine flow field
SHE	standard hydrogen electrode
STP	standard conditions with respect to temperature and pressure
T	temperature [K]

Greek letters

Δx	compressed felt thickness [m]
Δx_0	uncompressed felt thickness [m]
ε_0	porosity of uncompressed felt
ε_{cf}	porosity of compressed felt
$\kappa_{0\,333\,K}$	electrolyte ionic conductivity at 333 K [$S\,m^{-1}$]
κ	effective electrolyte conductivity (felt porosity and liquid hold-up correction) [$S\,m^{-1}$]
σ	Electronic conductivity [$S\,m^{-1}$]

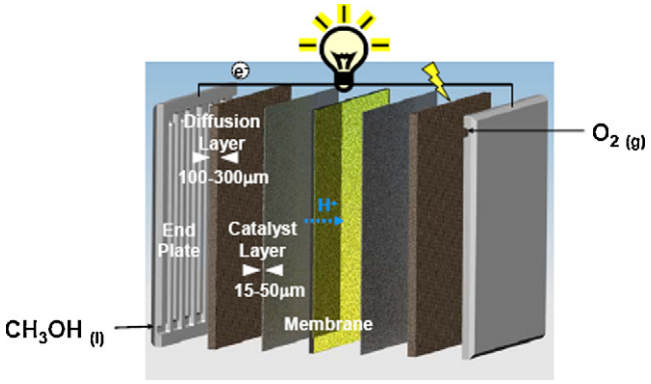

Fig. 1. Exploded view of DMFC with conventional GDE anode design.

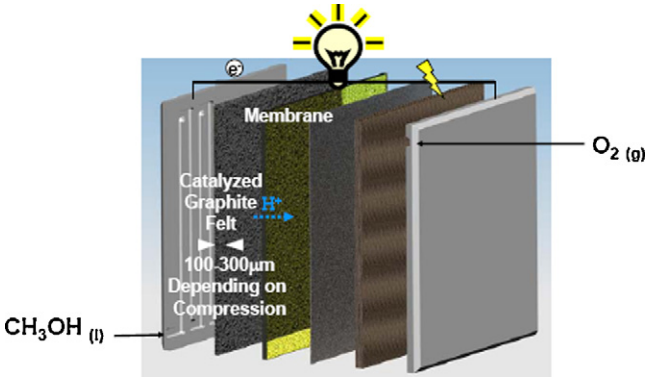

Fig. 2. Exploded view of DMFC with 3D extended reaction zone anode.

structures [18]. As shown in Table 1 the alternative anode structures generally provide significant improvements in fuel cell performance, compared to that obtained using conventional anodes. The observed peak superficial power densities ranged up to 2200 $W\,m^{-2}$. Note that comparisons among the different alternative designs are not recommended here because the performance of a DMFC is strongly influenced by variations in conditions such as the catalyst load, oxygen partial pressure, methanol concentration, flow and temperature—some of which are not recorded in the source articles. Further, one can assume that conventional channel type flow fields or flow beds were utilized, even though the respective flow fields were not described in detail in these papers.

In most work with DMFCs the anolyte is a solution of methanol in water, without a supporting electrolyte. The absence of a supporting electrolyte is desirable in so far as it simplifies operation of the fuel cell system and avoids unwelcome effluents. However, without a supporting electrolyte the ionic conductivity of the anode matrix depends on the relatively low conductivity of a solid polymer electrolyte, such as Nafion. This dependence limits the effective thickness of the anode matrix to about 20 μm and essentially constrains the anode to some variant of the GDE or CCM, which may not be an optimal solution for the design of a DMFC.

Our previous work aimed to improve the performance of DMFCs by employing an ionically conductive liquid anolyte in a conventional flow field with a highly porous electronically conductive anode, while extending the anode reaction zone thickness to 100–300 μm. As reported elsewhere [19] we were able to demonstrate a substantial increase in peak superficial power density over that of conventional CCMs by using an extended reaction zone anode (Fig. 2) consisting of graphite felt catalyzed by the surfactant assisted electro-deposition of PtRu and PtRuMo.

Now we present results of a more comprehensive study of the DMFC with its so-called 3D anode, in conjunction with both the

Table 1
Comparison of alternative and conventional DMFC anode designs. Conditions are indicated when specified in the source article.

Electrode area/catalyst load and composition	Reactants and conditions	Electrode design (1. alternative; 2. conventional)	Peak superficial power density [$W\,m^{-2}$]
9 cm^2 anode: 10 $g\,m^{-2}$ PtRu(1:1); cathode: 10 $g\,m^{-2}$ Pt	2 M CH_3OH + 0.5 M H_2SO_4; 12 $cm^3\,min^{-1}$; air, 1000 $cm^3\,min^{-1}$; ~100 kPa(abs); T = 363 K	1. PtRu on Ti mesh; 2. GDE (Vulcan XC-72) [14]	600; 700
(Area not specified) anode: 64 $g\,m^{-2}$ PtRu(1:1); cathode: 43 $g\,m^{-2}$ PtRu(1:1)	1 M CH_3OH; O_2	1. Cup-stacked carbon nanotubes; 2. GDE (Vulcan XC-72) [16]	900 (333 K), 1450 (363 K); 600 (333 K), 670 (363 K)
2 cm^2 anode: 30 $g\,m^{-2}$ PtRu(1:1); cathode: 50 $g\,m^{-2}$ Pt	2 M CH_3OH; 1 $cm^3\,min^{-1}$; O_2, 500 $cm^3\,min^{-1}$; T = 343 K	1. PtRu on porous hexagonal carbon support; 2. GDE (E-Tek) [17]	1700; 1200
2 cm^2 anode: 20 $g\,m^{-2}$ PtRu(1:1); cathode: 50 $g\,m^{-2}$ Pt	2 M CH_3OH; 1 $cm^3\,min^{-1}$; O_2, 500 $cm^3\,min^{-1}$; T = 333 K	1. PtRu on carbon nanocoils; 2. GDE (Vulcan XC-72); 2. GDE (E-Tek) [18]	2200; 1500; 1200

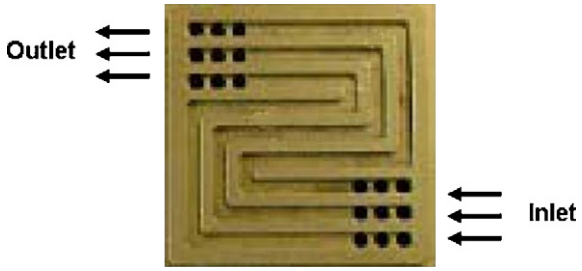

Fig. 3. Serpentine flow field incorporated into end plate (as supplied by Fideris Inc.).

standard fuel cell serpentine flow field of our previous work and a novel flow-by configuration similar to that used for electrosynthesis with gaseous reactants [20].

2. Experimental design

For the majority of published DMFC studies a single variable (e.g., temperature) was altered per experiment, while all other variables were kept nominally constant [17,18,21]. This univariate method of experimentation can lead to false conclusions, since interactions among two or more variables are not taken into account and in many cases there are no replications on which to base estimates of experimental variance. The present study uses both parametric and factorial experiments, first to establish appropriate values for the anode thickness and anolyte conductivity then to gauge the combined effects of methanol concentration, anolyte flow rate and temperature on the DMFC performance.

3. Experimental apparatus and procedures

The concept of the extended reaction zone (so-called 3D) anode for a DMFC is presented in Fig. 2, which also shows how methanol is fed to the anode of a single cell through a serpentine flow field incorporated into the backing plate, which acts as the current collector. The actual gold-plated stainless steel serpentine flow field used in this work is shown in Fig. 3 and has dimensions of 2.5 × 2.5 cm.

It was of interest to investigate alternatives to the serpentine flow field especially in conjunction with the three-dimensional anode. Figs. 4 and 5 show a flat current collector plate designed such that the anolyte flows upward through the porous graphite felt. In this case the anolyte and electric current pathways are predominantly orthogonal, corresponding to the so-called "flow-by" mode of operation [22]. Un-catalyzed graphite felt sections were also employed at the inlet and outlet to promote uniform fluid distribution across the anode chamber.

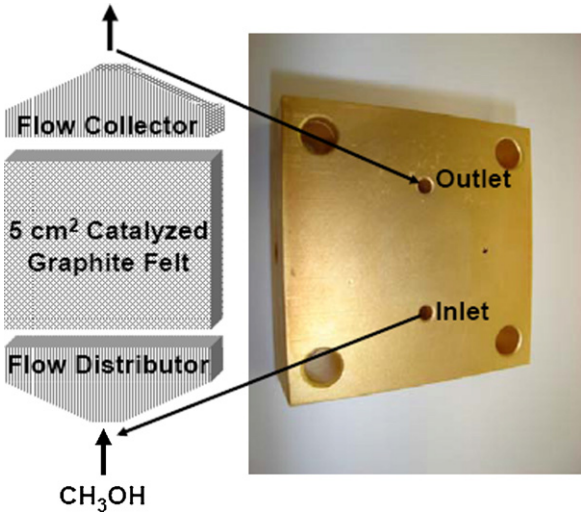

Fig. 4. Exploded view of flow-by anode schematic and photograph of flow-by type end plate.

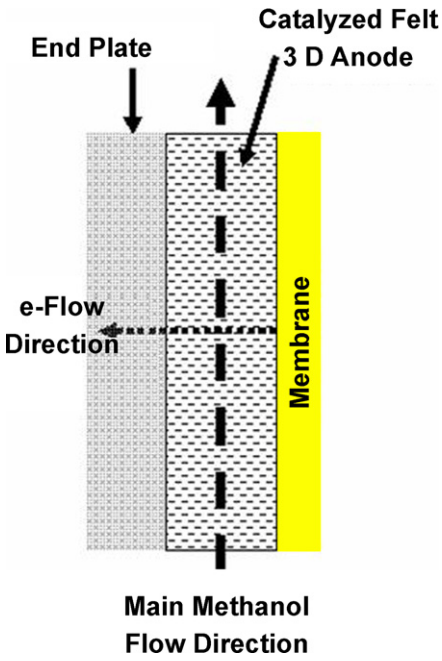

Fig. 5. Schematic of the flow-by anode concept.

For all experiments the anode substrate with a 5 cm^2 (2.24 cm × 2.24 cm) superficial area was graphite felt (GF-S3 from Test Solutions, Inc.) with ca. 20 μm diameter fibers and uncompressed thickness and porosity of, respectively 300 μm and 94%. Each felt was prepared for methanol electro-oxidation, as detailed elsewhere [19], by electro-deposition of catalyst nanoparticles onto the fibers. The atomic compositions and loadings for the PtRu and PtRuMo anode catalysts were, respectively 1.4:1, 43 g m^{-2} and 1:1:0.3, 52 g m^{-2}. A micrograph of the bare felt is shown in Fig. 6, along with a more magnified view of catalyst deposits on single fibers.

The catalyzed felts were enclosed in the fuel cell by a set of Teflon gaskets whose thickness was adjusted to fix the anode compression. Carbon cloths were placed as backing layers on both the anode (Textron, ca. 250 μm uncompressed thickness) and cathode (ELAT from E-Tek Inc., ca. 400 μm uncompressed thickness) microporous diffusion layer, side to ensure electronic contact of the entire electrode area. The anodes were installed in conjunction with the cathode catalyst (40 g m^{-2} Pt black) coated Nafion 117 membrane (180 μm thick from Lynntech Inc.) and the respective end plates, as indicated in Fig. 2. In operation the single fuel cell was coupled to a test station (Fideris Inc.) employing FC Power™ software to control the variables fuel cell temperature, oxidant flow rate, cathode pressure and current density. For all tests dry O_2 was supplied at a flow rate of 500 cm^3 min^{-1} STP and the cathode pressure was about 200 kPa(abs). The anolyte was a solution of methanol and sulfuric acid in water, delivered to the fuel cell in single pass mode at about 110 kPa(abs) by a peristaltic pump.

4. Results and discussion

4.1. Effect of three-dimensional anode compression and effective thickness

It was of interest to investigate the effect of compression on the DMFC polarization performance since the porosity, electronic

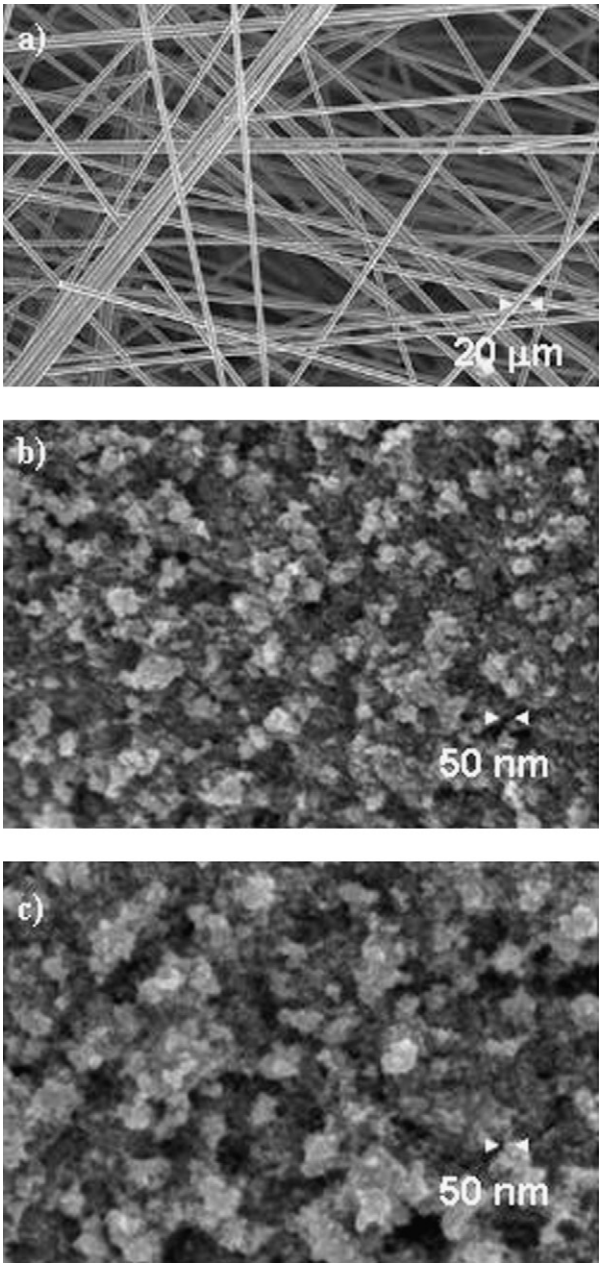

Fig. 6. Micrographs of un-catalyzed graphite felt (a) [19] (GF-S3) and PtRu (b) and PtRuMo (c) deposits on the graphite fiber surface [23].

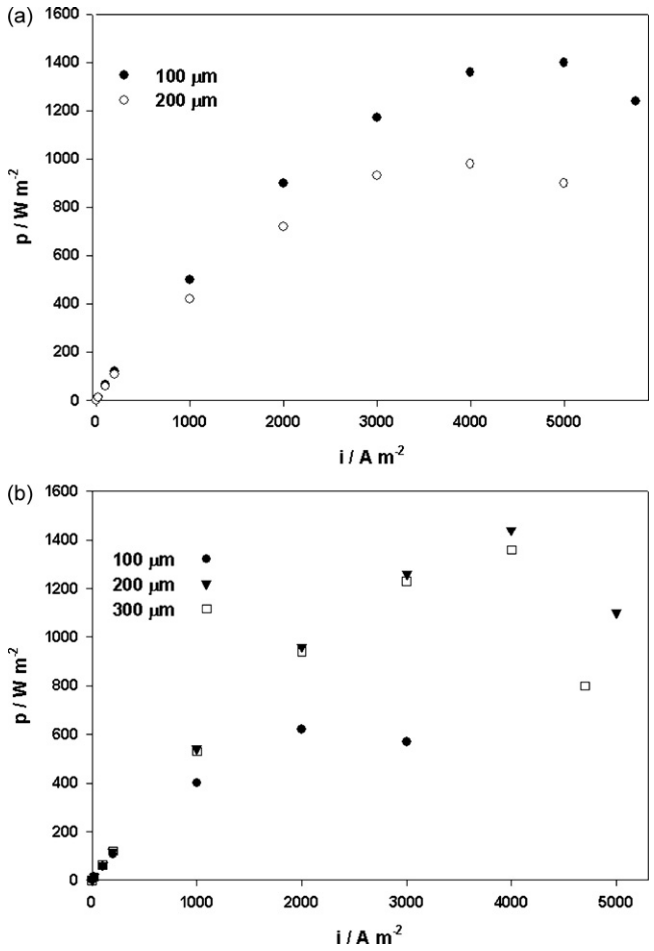

Fig. 7. Effect of anode thickness on the fuel cell performance using a serpentine flow field (a) or a flow-by design (b), anolyte: 1 M CH_3OH–0.5 M H_2SO_4, anolyte flow rate: 5 $cm^3\ min^{-1}$, T = 333 K. Anode catalyst = PtRu, loading = 43 $g\ m^{-2}$.

conductivity and contact resistance between the graphite felt and the current collector are all implicitly altered. Fig. 7 shows the effect of anode compression, expressed as the effective anode thickness (100, 200 and 300 μm) on the superficial power density of the DMFC using, respectively the standard serpentine and the flow-by configurations of the flow fields, under otherwise similar operating conditions.

Three features of these curves stand out for comment: (a) the performance of the fuel cell in both configurations is influenced by the compression and/or thickness of the anode, (b) for the standard flow field the performance improves when the anode thickness is decreased from 200 to 100 μm, whereas for the flow-by case the performance improves when the anode thickness is increased from 100 to 200 μm, and (c) with an anode thickness of 200 μm the flow-by configuration gave a higher peak power density (1420 $W\ m^{-2}$) than the standard flow field (1350 $W\ m^{-2}$).

These effects may be explained by the interaction of several phenomena that determine the potential, current and fluid flow distribution in a 3D electrode. The porosity and electronic conductivity of the anode are related to the degree of compression through Eqs. (1) and (2) [24] and the specific surface area of the bare fibers may be estimated by Eq. (3) [25]:

$$\varepsilon_{cf} = 1 - \frac{\Delta x_0(1-\varepsilon_0)}{\Delta x} \quad (1)$$

$$\sigma = 10 + 2800\left(1 - \frac{\varepsilon_{cf}}{\varepsilon_0}\right)^{1.55} \quad (2)$$

$$a_s = \frac{4(1-\varepsilon_{cf})}{d_f} \quad (3)$$

The dependence of the porosity, electronic conductivity and specific surface area of the bare felt (GF-S3) on its thickness is listed in Table 2.

Table 2
The effect of compression on GF-S3 graphite felt.

Thickness [μm]	Porosity	Electronic conductivity [$S\ m^{-1}$]	Volume specific surface area [$10^3\ m^2\ m^{-3}$]
100	0.83	131	35.0
200	0.91	29	17.5
300[a]	0.94	12	11.7

[a] Uncompressed.

It is clear from Fig. 7 that the thin 100 μm anode is beneficial only for the serpentine flow field, while the thicker 200–300 μm anodes gave better performance in case of the flow-by design. Using a gasket thickness of ~100 μm in conjunction with the flow-by end plate yielded relatively poor performance, due to a partial disintegration of the anode material resulting from compression.

For the serpentine flow field, the nominal thickness of the anode is influenced by the landings and channels since the felt can "expand" to some extent into the 1 mm deep channels. The expansion of the felt is more pronounced at a lower compression. Hence, the thicker anode has a less uniform contact with the current collector and higher effective resistance.

4.2. Effect of sulfuric acid concentration

The presence of a supporting electrolyte extends the effective thickness of a porous electrode approximately in proportion to the square root of the electrolyte conductivity. The sulfuric acid concentration is thus an important variable with respect to the performance of the three-dimensional anode. Fig. 8 shows the effect of the concentration of sulfuric acid in the anolyte (i.e., methanol solution) on the cell voltage and superficial power density of the DMFC with the serpentine flow field. These curves indicate an apparent optimum acid concentration around 0.5–1 M under the experimental conditions used here. Such a result may be rationalized by the interaction effects that determine the performance of the DMFC. First, the potential and current profile through the thickness of a 3D

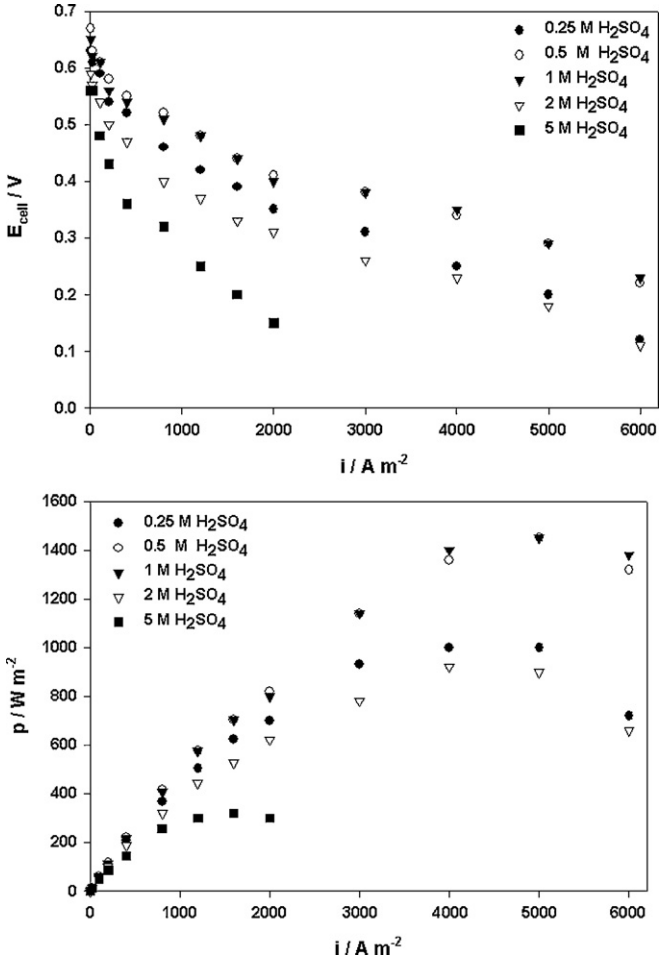

Fig. 8. Effect of anolyte sulfuric acid concentration on DMFC performance, anolyte: 1 M CH_3OH–x M H_2SO_4, anolyte flow rate: 5 cm^3 min^{-1}, T = 333 K. Serpentine flow field, nominal thickness = 1 mm.

Table 3
Ionic conductivity of H_2SO_4 solutions (T = 333 K, f = 0.83).

H_2SO_4 concentration [M]	Bulk conductivity [S m^{-1}]	Effective ionic conductivity [S m^{-1}]
0.25	12	9
0.5	29	22
1	55	42
2	96	73
5	120	91

electrode depends strongly on the ionic conductivity of the electrolyte, so that increasing the electrolyte conductivity lowers the internal Ohmic resistance and normally improves the performance of electrochemical reactors with 3D electrodes. Table 3 shows the bulk conductivity of sulfuric acid solutions and the corresponding effective conductivity in a 3D electrode of 83% porosity as estimated by the Bruggeman equation [26]:

$$\kappa = \kappa_0 (f)^{1.5} \quad (4)$$

On the contrary, increasing the H_2SO_4 concentration may promote methanol crossover by diffusion and electro-osmotic drag and hinder methanol mass transfer by increasing the anolyte viscosity. A more subtle consequence of increasing the acid concentration is the specific adsorption of sulfate anions onto the anode catalyst that can slow the competitive electro-oxidation of methanol [27]. The most favorable acid concentration of 0.5–1 M corresponds to the condition where the various effects are balanced. Note that Fig. 8 represents a univariate experiment, which means the optimum acid concentration may shift with changes in factors such as the anode porosity, methanol concentration and temperature.

4.3. Factorial experiments

A factorial experimental design strategy was implemented to study the PtRu and PtRuMo catalyzed graphite felt anodes employing both the serpentine and flow-by feeding modes. Based on the observations of Sections 4.1 and 4.2 the effective anode thickness was 100 μm for the serpentine flow field and 200 μm for the flow-by feeder, respectively. The sulfuric acid concentration was 0.5 M throughout. Table 4 lists the variables of the factorial design at their high (+1), low (−1) and center point (0) levels. For each catalyst and flow field design the first experiment was carried out at center point conditions. The rest were conducted in a random sequence and the replicate runs were done after completion of the full factorial. For each sequence of tests starting with the center point conditions a fresh cathode and anode were used. Preparing a fresh anode for every single polarization experiment would have been prohibitively expensive and time consuming.

Considering the peak superficial power density as the response variable, Fig. 9 presents the factorial results in cube plots and Table 5 summarizes the statistical effects and interactions of the three variables.

Fig. 9 shows that regardless of the flow configuration, at the high level of the variable temperature (Table 4) the PtRuMo catalyst performed better than PtRu, confirming previous fundamental studies from our group showing the temperature activation effect of the Mo [19]. For each catalyst and end plate design the highest peak

Table 4
Variables and their levels in factorial DMFC experiments.

Level	Methanol concentration, c (M)	Anolyte flow rate, F (cm^3 min^{-1})	Fuel cell temperature, T (K)
+1	2	10	353
0	1.25	6	333
−1	0.5	2	313

Table 5
Statistical effects from factorial experiments.

Catalyst	Flow mode	Main effects			Interactions			CI[a]	Curvature	CI[a]
		c	*F*	*T*	*c*–*F*	*c*–*T*	*F*–*T*			
PtRu	Serpentine	315	−50	1145	−40	35	−90		123	
PtRu	Flow-by	328	−93	1106	−63	58	−143		168	
PtRuMo	Serpentine	273	−28	1458	3	48	−103	99	65	95
PtRuMo	Flow-by	293	−73	1448	13	63	−153		86	

[a] CI = 95% confidence interval (+/−), estimated from pooled variance of all 28 replicates.

power density was obtained with the flow rate at the low level and temperature as well as concentration at the high level (Fig. 9). The peak power density under these conditions was observed at ~7000 A m^{-2} for both catalysts and flow modes. The highest superficial peak power density was 2380 W m^{-2} for operation in flow-by mode at 353 K using 2 M methanol at a flow rate of 2 cm^3 min^{-1} with a PtRuMo catalyst, while PtRu yielded 2240 W m^{-2} under the same conditions (Fig. 9).

The effects of the three main factors (*c*, *F* and *T*) are mostly related to electrode kinetics, mass transfer and membrane transport phenomena. Increasing methanol concentration, anolyte flow and/or temperature raises the intrinsic rate of the anode reaction and the methanol mass transfer limiting current density, which tends to improve the fuel cell performance. However, these effects are countered by an increase in the methanol crossover flux that results from the higher methanol concentration gradient, combined with increased membrane permeability at a higher temperature. Higher anolyte flows also raise the anode pressure and possibly enhance the flux of methanol across the membrane.

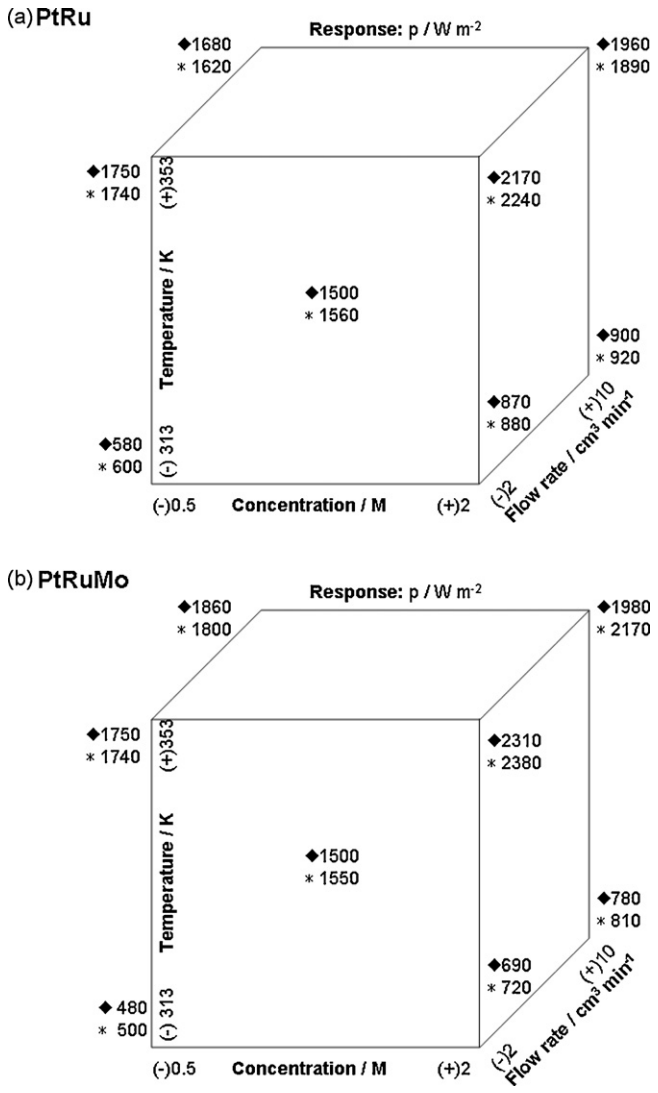

Fig. 9. Cube plots of peak power density as a function of methanol concentration, flow rate and temperature for PtRu (a) and PtRuMo (b) catalyzed 3D anodes using either the serpentine flow field (♦) or the flow-by mode (*).

Table 5 shows that the most pronounced impact of the flow field design for both catalysts, was related to the main effect of the flow rate (*F*) and to the flow rate–temperature interaction effect (*F*–*T*). For example, in case of the PtRu catalyst switching from the serpentine to the flow-by mode and operating at high flow rate decreased the peak power output by 93 W m^{-2} compared to a decrease of 50 W m^{-2} in case of serpentine design. While the absolute values are smaller than the required 95% confidence level (i.e., 99 W m^{-2}), the trends are very consistent for the two types of feeders employed. Further, the difference between serpentine and flow-by modes was accentuated at high temperature, as shown by the *F*–*T* values for the flow-by configuration of −143 and −153 W m^{-2} for PtRu and PtRuMo, respectively (Table 5). Due to the consistently negative interaction effect between flow rate and temperature, operating at both high flow rate and high temperature is disadvantageous for the peak power output. This result is probably due to the competition between the rate of anodic methanol oxidation and its rate of loss to the cathode, in which the combination of high flow and high temperature favors the crossover relative to the anode reaction [3].

The data of Table 5 also show a significant curvature in the effects of *c*, *F* and *T* for the PtRu catalyst. Interestingly, the curvature effect was again consistently higher for the flow-by mode of operation. Curvature points to non-linearity in the response (*p*) of the DMFC to changes in the levels of the factorial variables *c*, *F* and *T*. This result implies that significant improvements in the performance of the fuel cell could potentially be made by a more thorough examination of the three factor experimental space. Such an investigation should include changes to the anode aspect ratio and liquid distributor to improve mass transfer and to drive CO_2 gas out of the anode in 2-phase flow with the anolyte [25]. Consideration should also be given to transverse dispersion across the anode thickness. In this respect, previous studies of transverse dispersion in graphite felt flow-by "electrodes" [28] indicate that the combined effects of dispersion and potential distribution might be exploited to suppress methanol crossover by manipulating the methanol concentration profile in the anode. The high superficial power densities reported in Fig. 9 support the notion that the three-dimensional anode helps to disengage CO_2 and/or suppresses methanol crossover. Both effects, in synergy with the improved catalyst activity, could contribute to the improved performance compared to the conventional CCM.

As well as the superficial power density (W m^{-2}) reported above, the volumetric power density (W m^{-3}) is an important metric of fuel cell performance. Clearly, the employment of an extended surface anode can decrease the volumetric power density in proportion to the extra thickness of the cell. However, in the case of the flow-by system the anode flow field is effectively eliminated, with a corresponding reduction of about 1 mm in the cell thickness.

Table 6
Previous studies of effects of methanol concentration, anolyte flow and temperature on DMFC operation.

Source	Electrode area and catalyst	Reactants and conditions	Observations
[29]	25 cm^2 anode: PtRu 15 $g\,m^{-2}$; cathode: Pt 10 $g\,m^{-2}$	c = 0.5–3 M; F = 2 $cm^3\,min^{-1}$; $F(O_2)$ = 150 $cm^3\,min^{-1}$; T = 323–353 K	Maximum peak power density: 380 $W\,m^{-2}$ at 353 K obtained with 1 M CH_3OH
[21]	(Area not specified) anode: PtRu 30 $g\,m^{-2}$; cathode: Pt 30 $g\,m^{-2}$	c = 0.5–6 M; F = 0.5–10 $cm^3\,min^{-1}$; F(air) = 600 $cm^3\,min^{-1}$ STP; T = 343 K	Membrane methanol permeability increases with temperature. Performance improves with increasing anolyte flow rate. Maximum peak power density: 750 $W\,m^{-2}$ obtained with 1–2 M CH_3OH.
[30]	5 cm^2 anode: PtRu 40 $g\,m^{-2}$; cathode: Pt 40 $g\,m^{-2}$	c = 0.5–4 ; F = 1–9 $cm^3\,min^{-1}$; $F(O_2)$ = 200 $cm^3\,min^{-1}$; ~100 kPa(abs); T = 313–353 K	Maximum peak power density: 2250 $W\,m^{-2}$ at 353 K obtained at 3 $cm^3\,min^{-1}$, with 1 M CH_3OH. Performance dropped at low and high flow rates.
[31]	5 cm^2 anode: PtRu 40 $g\,m^{-2}$; cathode: Pt 40 $g\,m^{-2}$	c = 0.5–2 M; F = 0.15–5 $cm^3\,min^{-1}$; F(air) = 100 $cm^3\,min^{-1}$; ~100 kPa(abs); T = 313–353 K	Fuel conversion and power output increased with decreasing anolyte flow rate. At 353 K the performance dropped for c > 1 M CH_3OH

Considering only the active area of the electrodes, with bipolar flow field plates 3 mm thick in the conventional mode, the peak superficial power densities of Fig. 9 extrapolate to volumetric power densities in fuel cell stacks, with dual serpentine flow fields and with flow-by anodes, respectively, of about 650 and 850 $W\,l^{-1}$. The penalty for the increased volumetric power density in the flow-by mode would probably be a higher pressure drop through the anode.

Table 6 summarizes literature results regarding the effects of methanol concentration, anolyte flow and temperature on the behavior of DMFCs. In all studies an improvement in performance resulted from an increase in the operating temperature, which is also in agreement with data presented by Chai et al. [17] and Hyeon et al. [18]. With respect to the separate effects of methanol concentration, anolyte flow rate and temperature the results of Table 5 are largely in agreement with those of the previous studies listed in Table 6. However, the interpretation and comparison of these data is bedeviled by inconsistent experimental conditions, which are also not always completely specified.

5. Conclusions

Experiments in a 5 cm^2 single cell DMFC showed that an extended reaction zone three-dimensional anode is a promising alternative design with either a conventional serpentine feeder plate or using a novel flow-by configuration. The presence of a supporting electrolyte in the 3D electrode allows extension of the electro-active thickness of the catalyzed graphite felt anode to about 300 μm, with a high porosity (80–90%). With maximizing the peak superficial power density as the primary objective, univariate experiments indicated that the optimum sulfuric acid supporting electrolyte concentration was about 0.5–1 M. This narrow concentration range balances the contrary effects of electrolyte conductivity and methanol crossover on the power output of the DMFC. Factorial experiments with an 0.5 M acid anolyte in a nominally 200 μm thick anode show that the PtRuMo catalyst yielded better performance than the PtRu at a high temperature (353 K) whereas the PtRu catalyst outperformed the PtRuMo at a low temperature (313 K).

Further, at the scale and conditions of this work factorial experiments revealed that the flow-by anode configuration gave marginally better performance than a conventional serpentine flow field, with a peak superficial power density reaching $2380 \pm 100\,W\,m^{-2}$ at 7000 $A\,m^{-2}$, corresponding to a volumetric power density of about 850 $W\,l^{-1}$. This is the first investigation the authors are aware of that employs a statistically designed experimental strategy to evaluate the interacting effects among key variables affecting the direct methanol fuel cell performance. Such an experimental strategy is of paramount importance as a basis for modeling, optimizing and engineering fuel cell systems.

Acknowledgements

The authors gratefully acknowledge funding from the BC Advanced Systems Institute and the Natural Sciences and Engineering Research Council of Canada, together with the support of the University of British Columbia.

References

[1] H.K. Lee, J.H. Park, D.Y. Kim, T.H. Lee, J. Power Sources 131 (2004) 200–206.
[2] V.M. Barragán, C. Ruiz-Bauzá, J.P.G. Villaluenga, B. Seoane, J. Power Sources 130 (2004) 22–29.
[3] A. Casalegno, P. Grassini, R. Marchesi, Appl. Therm. Eng. 27 (2007) 748–754.
[4] D.P. Wilkinson, M.C. Johnson, K.M. Colbow, S.A. Campbell, Method and apparatus for reducing reactant crossover in a liquid feed electrochemical fuel cell, U.S. Patent 5,874,182 (23 February 1999).
[5] A. Lam, D.P. Wilkinson, J. Zhang, Electrochem. Soc. Trans. 1 (2006) 273–281.
[6] N. Miyake, J.S. Wainright, R.F. Savinell, J. Electrochem. Soc. 148 (2001) A898–A904.
[7] R. Jiang, H.R. Kunz, J.M. Fenton, J. Membr. Sci. 272 (2006) 116–124.
[8] D. Kim, M.A. Scibioh, S. Kwak, I.-H. Oh, H.Y. Ha, Electrochem. Commun. 6 (2004) 1069–1074.
[9] P. Argyropoulos, K. Scott, W.M. Taama, Electrochim. Acta 44 (1999) 3575–3584.
[10] K. Scott, P. Agyropopoulos, P. Yiannopoulos, W.M. Taama, J. Appl. Electrochem. 31 (2001) 823–832.
[11] P. Argyropoulos, K. Scott, W.M. Taama, J. Appl. Electrochem. 29 (1999) 661–669.
[12] J. Nordlund, A. Roessler, G. Lindbergh, J. Appl. Electrochem. 32 (2002) 259–265.
[13] T. Bewer, T. Beckmann, H. Dohle, J. Mergel, D. Stolten, J. Power Sources 125 (2004) 1–9.
[14] R.G. Allen, C. Lim, L.X. Yang, K. Scott, S. Roy, J. Power Sources 143 (2005) 142–149.
[15] Z.-G. Shao, F. Zhu, W.-F. Lin, P.A. Christensen, H. Zhan, Phys. Chem. Chem. Phys. 8 (2006) 2720–2726.
[16] C. Kim, Y.J. Kim, Y.A. Kim, T. Yanagisawa, K.C. Park, M. Endo, M.S. Dresselhaus, J. Appl. Phys. 96 (2004) 5903–5905.
[17] G.S. Chai, S.B. Yoon, J.S. Yu, J.H. Choi, Y.E. Sung, J. Phys. Chem. B 108 (2004) 7074–7079.
[18] T.S. Hyeon, S. Han, Y.-E. Sung, K.-W. Park, Y.-W. Kim, Angew. Chem., Int. Ed. 42 (2003) 4352–4356.
[19] A. Bauer, E.L. Gyenge, C.W. Oloman, J. Power Sources 167 (2007) 281–287.
[20] C. Oloman, B. Lee, W. Leyten, Can. J. Chem. Eng. 68 (1990) 1004–1009.
[21] J. Ge, H. Liu, J. Power Sources 142 (2005) 56–69.
[22] F.C. Walsh, A First Course in Electrochemical Engineering, The Electrochemical Consultancy, United Kingdom, 1993, p. 246.
[23] A. Bauer, E.L. Gyenge, C.W. Oloman, Electrochim. Acta 51 (2006) 5356–5364.
[24] C. Oloman, M. Matte, C. Lum, J. Electrochem. Soc. 138 (1991) 2330–2334.
[25] I. Hodgson, C. Oloman, Chem. Eng. Sci. 54 (1999) 5777–5786.
[26] G. Prentice, Electrochemical Engineering Principles, Prentice Hall, Eaglewood Cliffs, New Jersey, 1991, p. 213.
[27] A.V. Tripkovic, K.D. Popovic, Electrochim. Acta 41 (1996) 2385–2394.
[28] L. Gao, Dispersion in three-dimensional electrodes, M.A.Sc. Thesis, The University of British Columbia, Vancouver, BC, 2000, pp. 107–114.
[29] G.-B. Jung, A. Su, C.-H. Tu, F.-B. Weng, J. Fuel Cell Sci. Technol. 2 (2005) 81–85.
[30] S.H. Seo, C.S. Lee, Energy Fuels 22 (2008) 1212–1219.
[31] B. Gurau, E.S. Smotkin, J. Power Sources 112 (2002) 339–352.